Science of the Total Environment 642 (2018) 733–741

Contents lists available at ScienceDirect

Science of the Total Environment

journal homepage: www.elsevier.com/locate/scitotenv

Canopy and understory nitrogen addition increase the xylem tracheid size of dominant broadleaf species in a subtropical forest of China

Xinyu Jiang [a,b], Nan Liu [a], Xiankai Lu [a], Jian-Guo Huang [a,*], Jiong Cheng [b], Xiali Guo [a], Shuhua Wu [a]

[a] Key Laboratory of Vegetation Restoration and Management of Degraded Ecosystems, Guangdong Provincial Key Laboratory of Applied Botany, South China Botanical Garden, Chinese Academy of Sciences, Guangzhou 510650, China
[b] Guangdong Key Laboratory of Integrated Agro-environmental Pollution Control and Management, Guangdong Institute of Eco-environmental Science & Technology, Guangzhou 510650, China

HIGHLIGHTS

- N addition increased xylem tracheid size of dominant broadleaf species in Southern China.
- Effect of N addition on the xylem anatomy was dependent on N addition approaches.
- Understory N addition did not fully simulate canopy N deposition.
- Tree growth of broadleaf species was not affected by canopy or understory N addition.

GRAPHICAL ABSTRACT

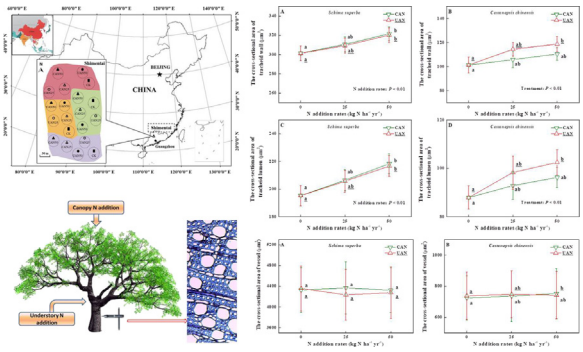

ARTICLE INFO

Article history:
Received 11 April 2018
Received in revised form 11 June 2018
Accepted 11 June 2018
Available online 17 June 2018

Editor: Elena PAOLETTI

Keywords:
Canopy nitrogen addition
Subtropical broadleaf species
Xylem anatomy
Tracheid
Vessel

ABSTRACT

Tree xylem anatomy is associated with carbon accumulation and wood quality. Increasing nitrogen (N) deposition can cause a significant effect on xylem anatomy, but related information is limited for subtropical broadleaf tree species. A 3-year field N addition experiment, with different N addition approaches (canopy and understory) and addition rates (0, 25, and 50 kg N ha^{-1} yr^{-1}), was performed beginning in 2013 in a subtropical forest of China. N addition effects on xylem tracheid (wall and lumen) size, vessel, and growth of dominant broadleaf species (*Schima superba Gardn. et Champ.* and *Castanopsis chinensis* (*Sprengel*) *Hance*) were investigated. The results showed that The effect of N addition on tracheid size was dependent on the tree species and addition approaches. Canopy N addition did not affect the tracheid size of *C. chinensis*, while both addition approaches increased the tracheid size of *S. superba*. The vessel size of both species was not affected by N addition. There was no difference in radial growth or other growth-related variables between the control and N-treated trees. These findings indicated that short-term N addition could significantly affect xylem anatomy, but might not influence tree growth. Meanwhile, understory N addition may pose challenges for mechanistic understanding and forest dynamics projection.

1. Introduction

Atmospheric CO_2 can be captured and converted to structural carbohydrates as newly formed xylem components (tracheid and vessel) in trees (Rossi et al., 2016). Xylem formation is one of the strongest C

* Corresponding author.
E-mail address: huangjg@scbg.ac.cn (J.-G. Huang).

https://doi.org/10.1016/j.scitotenv.2018.06.133
0048-9697/

sinks in trees, making xylem formation a vital process of C accumulation in forest ecosystems (Huang et al., 2014). On the other hand, xylem contributes to the transport system and provides structural support; therefore, the xylem characteristics (e.g. tracheid size, vessel size and fiber dimensions) can affect water transport efficiency, wood quality, and tree resistance to drought (Lachenbruch and McCulloh, 2014; Santini et al., 2016). Concurrently increasing atmospheric N deposition (resulting from fossil-fuel combustion and agricultural fertilization) is likely to affect the xylem anatomy and productivity of forest trees (Thomas et al., 2010; Ibanez et al., 2016). However, most previous studies about the N effects on xylem anatomy and productivity were conducted in boreal or temperate forests (N-limited ecosystems), and largely focused on coniferous tree species (Makinen et al., 2002; Zhao and Liu, 2009; Rossi et al., 2016). Information about the effect of N deposition on the xylem anatomy of the broadleaf tree species in subtropical or tropical forests is limited. Current N deposition rates in the subtropical region of China range from 15 to 73 kg N hm^{-2} yr^{-1} (Lu et al., 2014; Lu et al., 2015) and are projected to continuously increase in the coming decades (Galloway and Cowling, 2002). Therefore, it is necessary to investigate the effect of N deposition on the xylem anatomy of broadleaf species in subtropical forests.

Tree wood is formed through a series of processes, including cell division, expansion, cell wall lignification, and cell maturation (Samuels et al., 2006). The mechanical properties of tree wood are closely associated with the physical structure of xylem (Pratt et al., 2007; Onoda et al., 2010), which further determines the suitability of tree wood in the wood-processing industry. The xylogenesis process and the anatomical properties of wood (i.e., cell size, wall-thickness) are strongly influenced by many environmental factors, such as nutrients (Hacke et al., 2010) and water (Arend and Fromm, 2007). Hacke et al. (2010) reported that N addition could increase the vessel size and water conductivity of a hybrid poplar. Previous studies have reported positive (Hutchison and Henry, 2010) or insignificant (Dao et al., 2015) effects of increased N availability on xylogenesis, xylem anatomy, and tree growth. In boreal forests, low nutrient availability (mainly N) has been identified as a key limiting factor for tree growth (Lukac et al., 2010). For boreal trees, elevated N availability can increase xylem tracheid size due to increased photosynthetic rates, higher transpiration requirements, and prolonged mitotic activity (Hawkins et al., 1995; Beets et al., 2001; Makinen et al., 2002). In contrast to temperate or boreal forests, subtropical and tropical forests are not N-limited ecosystems with higher soil N availability and faster N cycling rates (Wright et al., 2011; Brookshire et al., 2012). Subtropical and tropical forests contribute greatly to the regional or biome C cycle (Findlay, 2005; Townsend et al., 2011). The potential changes in xylem anatomy of subtropical broadleaf tree species following increasing N deposition may substantially influence forest productivity.

Most past and ongoing experiments about N deposition effects on tree growth were conducted using understory N addition or with high amounts of added N (May et al., 2005; Hogberg et al., 2006; Talhelm et al., 2013; Zhang et al., 2015), which could not simulate natural N deposition (deposited above the canopy layer). Naturally deposited N passes through the canopy layer first before it reaches the forest floor, and the composition of inorganic N will be changed during this process (Houle et al., 2015). Meanwhile, chemical retention in the bark, immobilization in dead organic matters, and volatilization as a gaseous state can lead to less availability of deposited N to plants (Hanson and Lindberg, 1991; Dail et al., 2009; Matson et al., 2014). Therefore, it is necessary to compare the potential impacts of different N addition approaches (canopy and understory N addition) on xylem anatomy and tree growth.

This study aims to test the effects of different N addition approaches (canopy and understory N addition) and different N addition rates on the xylem anatomy of the broadleaf tree species in subtropical forests. We aim to investigate 1) how N addition affects xylem anatomy of broadleaf species and 2) how xylem anatomy and tree growth respond to different approaches of N addition. To fill these knowledge gaps, a 3-year field N addition manipulative experiment has been performed in a subtropical forest of southern China beginning in 2013.

2. Materials and methods

2.1. Field experimental design

In our study, a field N manipulative experiment was conducted in the Shimentai National Nature Reserve (24°22′-24°31′ N, 113°05′-113°31′ E) of Guangdong Province, in southern China. The study site is dominated by a subtropical monsoon climate with alternate dry and moist seasons. In this region, annual rainfall and temperature are 2364 mm and 20.8 °C, respectively. The forest type belongs to evergreen broadleaf forest, and the tree species in the study site include *S. superba*, *C. chinensis*, *Cryptocarya concinna Hance*, *Machilus chinensis* (*Champ. ex Benth.*) *Hemsl.*, and *Engelhardia roxburghiana Wall.* In southern China, *S. superba* and *C. chinensis* are two dominant broadleaf tree species widely distributed in subtropical forests. In general, *S. superba* grows in relatively nutrient-poor soils, whereas *C. chinensis* grows in relatively nutrient-rich soils (Kong et al., 1997; Mo et al., 2008). The forest age is 50 (thinned in 1965) with a stand density of 818 tree ha^{-1}. Trees with a diameter at breast height (DBH) ≥ 10 cm were investigated on July 2012. Mean tree DBH and tree height are 18.6 cm and 13.8 m, respectively. Soil type in this region is latosolic red soil with a pH from 5.0 to 5.5. Subtropical forests are not N-limited ecosystems compared with P availability, with high soil N availability, rapid rates of N cycling, and the lack of N limitation to NPP (Hedin et al., 2009; Wright et al., 2011; Brookshire et al., 2012). Forests in this region are not N-limited compared with most temperate and boreal ecosystems (Mo et al., 2008; Lu et al., 2010; Lu et al., 2013). Indeed, soils in these ecosystems are highly weathered, with low base cation concentrations and high Al concentrations (Lu et al., 2014). In recent measurements, the N deposition rate of this region was 34.1 kg N ha^{-1} yr^{-1} (Zhang et al., 2015), comparable to the highest levels of N deposition occurring in Europe (MacDonald et al., 2002). Therefore, 25 kg N ha^{-1} yr^{-1} was chosen as the medium level of the N addition rate in our study, which was close to the N deposition rate of this region.

The field N addition experiment includes two N addition approaches, canopy N addition (CAN) and understory N addition (UAN). This experiment is designed with five different N treatments, which include: 1) CAN of 25 kg N ha^{-1} yr^{-1} (CAN25), 2) CAN of 50 kg N ha^{-1} yr^{-1} (CAN50), 3) UAN of 25 kg N ha^{-1} yr^{-1} (UAN25), 4) UAN of 50 kg N ha^{-1} yr^{-1} (UAN50), and 5) control (CK, without N addition). Within the study site, four blocks were established, and five treated plots (represented as five different N treatments) were randomly assigned within each block. The area of each circular plot is 907 m^2 with a radius of 17 m. Treated plots were separated by a 20 m buffer zone to minimize contamination of the N solution between plots. The location of Shimentai National Nature Reserve and the experimental design of field N addition were listed in Fig. 1.

The N addition experiment was initiated in April 2013. For CAN, a supporting tower was installed in the center of each CAN-treated plot. The supporting tower is 35 m high and a canopy spraying system, which was used to deliver the N solution, was installed on the top of the tower (above the forest canopy). The canopy spraying system includes 4 sprinklers (with different spraying ranges), which can turn 360° and spray the solution as far as 17 m. N addition events were performed monthly from April to October (the growing season of this forest) each year (Zhang et al., 2015). The application of solution was at a rate of 3 mm precipitation, equivalent for each addition event, and the total additional solutions account for <1% of the total annual precipitation of our study site. All the technical parameters and operations were controlled by a central computer. NH_4NO_3 was used as N source and mixed with surface water drained from a nearby lake. Lake water was sampled and analyzed before each N addition event to ensure the

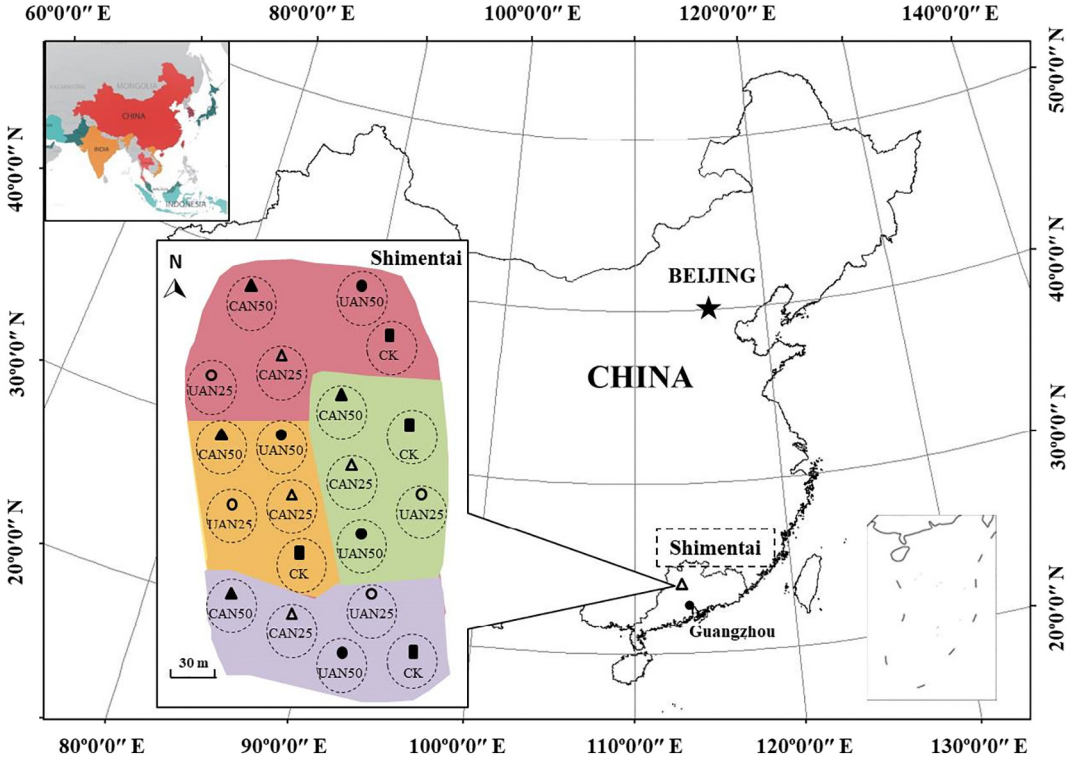

Fig. 1. Location of the experimental site and experimental design of different N treatments. CAN and UAN represent canopy addition N and understory addition N manipulative experiments, respectively. CK represents treatment without N addition. Numbers of 25 and 50 represent N addition rates of 25 kg N ha^{-1} yr^{-1} and 50 kg N ha^{-1} yr^{-1}, respectively. The four colors represent 4 blocks, and each circle represents each treated plot.

target N concentration. The total organic C, N, P, and K concentrations of lake water were 0.79 ± 0.20 mg L^{-1}, 0.62 ± 0.16 mg L^{-1}, 2.12 ± 1.20 μg L^{-1}, and 0.30 ± 0.06 mg L^{-1}, respectively. N addition events were all conducted in the morning or evening when wind speed was <1 m s^{-1} with minimal sunshine. For UAN, N solutions were sprinkled 1.5 m above the forest ground using automatic irrigation systems. The automatic irrigation system, including 5 sprinklers, was installed in each UAN-treated plot, and 5 sprinklers were evenly distributed in the plot.

Natural N deposition includes both dry and wet deposition, and the composition of deposited N includes both NH_x (NH_3, R-NH_2, and NH_4^+) and NO_x. Meanwhile, the amount of deposited N is evenly distributed in different dates (Zhang et al., 2015). For CAN treatment of our study site, N is artificially deposited through wet deposition once per month, and the composition of deposited N only includes NH_4^+ and NH_3^- (Zhang et al., 2015). These are the major differences between CAN treatment and natural N deposition. In each plot, one *S. superba* and one *C. chinensis*, with a healthy overall appearance and similar growth pattern, were selected as target trees. The photosynthetic rate, stomatal conductance, cellulose $\delta^{13}C_{PDB}$, and microcores were measured or sampled on these target trees. However, for diameter at breast height (DBH) measurements, all *S. superba* and *C. chinensis* with DBH ≥ 10 cm were measured.

2.2. Diameter at breast height, photosynthetic measurement, and stomatal conductance

Before the setup of the N addition experiment, trees with DBH ≥ 10 cm were first investigated within each plot on July 2012. Initial DBHs of *S. superba* and *C. chinensis* were collected from that data set. Red paint was used to mark the measured position on the surface of the tree stem for DBH measurement in the future. On July 2016, a second DBH measurement of *S. superba* and *C. chinensis* was carried out based on the red paint mark on the surface of stem using a caliper when microcores were sampled. DBH increments (3 years) of *S. superba* and *C. chinensis* were calculated by subtracting the second measured value from the first one. There were 16, 15, 9, 9, and 12 measured *S. superba* in CK, CAN25, CAN50, UAN25, and UAN50 treatments, respectively. There were 24, 20, 27, 33, and 24 measured *C. chinensis* in CK, CAN25, CAN50, UAN25, and UAN50 treatments, respectively.

Leaf photosynthetic rates of *S. superba* and *C. chinensis* were measured on clear days on July 2016 using a LI-6400 portable photosynthesis analyzer (LI-COR, Lincoln, NE, USA) according to the method of Liu et al. (2016). Supporting towers installed in treatment plots were used to access the foliage. For target trees, 4 to 5 healthy leaves (both included sun leaves and shade leaves) were used for photosynthetic rate measurements. Fully expanded leaflets and leaf-blade sections were enclosed in a reference chamber under constant conditions (500 cm^3 min^{-1} air flow; 400 μmol mol^{-1} CO_2 concentration; 1500 μmol m^{-2} s^{-1} light intensity; ambient air humidity; ambient O_2 concentration; 28 °C leaf temperature). A-PPFD curves were fitted in order to calculate the leaf photosynthetic rates (Liu and Guo, 2012). Stomatal conductance data were automatically obtained simultaneously with the photosynthesis measurements using an LI-6400 analyzer.

2.3. Cellulose extraction and $\delta^{13}C_{PDB}$ analysis

Plant materials used for cellulose $\delta^{13}C_{PDB}$ analysis were sampled from each target tree on July 2016. Woodchips were collected from the trunk surface of each target tree using a billhook. Cellulose of woodchip was extracted according to the following method (Loader et al., 1997): All woodchips were first dried at 70 °C for 24 h and then cut into small slivers (~40 μm thick) using a razor blade. After that, 1 g wood slivers were placed into a Soxhlet extraction vessel containing 175 mL deionized water (room temperature), 2.5 g sodium chlorite, and 1.7 mL acetic acid. The vessel was then covered with a watch glass and placed in an ultrasonic bath at 70 °C for 4 h. After each hour, 2.5 g sodium chlorite and 1.7 mL acetic acid were added to the vessel.

After the ultrasonic bath, the solution was filtered through vacuum filtration, and the residual was successively washed with 50 mL hot deionized water (70 °C) and 50 mL deionized water (room temperature). Again, 75 mL 10% (w/v) sodium hydroxide was added to the vessel, and then the vessel was placed in the ultrasonic bath at 80 °C for 45 min. After the ultrasonic bath, the solution was filtered by vacuum filtration, and the residual was washed with 50 mL cold deionized water (at room temperature). After that, 70 mL 17% (w/v) sodium hydroxide was added to the vessel, and then the vessel was placed in the ultrasonic bath at room temperature for 45 min. After the ultrasonic bath, the solution was filtered by vacuum filtration, and the residual was successively washed with 20 mL 17% sodium hydroxide solution, 100 mL deionized water (room temperature), and 20 mL 1% (w/v) hydrochloric acid. Finally, 100 mL deionized water (room temperature) was used to wash the residual. Extracted cellulose was then dried in a vacuum oven for 5 h. C content and $\delta^{13}C_{PDB}$ of extracted cellulose were determined using an isotope ratio mass spectrometer (Isoprime 100, Isoprime Ltd., UK) in the public laboratory of South China Botanical Garden, Chinese Academy of Sciences.

2.4. Xylem anatomy

Dominant *S. superba* and *C. chinensis* were chosen as target species. Related characteristics of these two dominant species can be found in Table 1. On July 2016 (after 3 years of the N addition experiment), wood microcores of target trees were sampled from the stem at 1.3 m aboveground using a Trephor instrument (University of Padova, Padova, Italy) (Rossi et al., 2006). All microcores were sampled from the same orientation to avoid sunshine and slope aspect effects on xylem cell formation. All microcores were approximately 1 cm length and 2 mm width. The microcore was placed in an Eppendorf microtube containing 50% aqueous ethanol solution and stored at 4 °C after collection. Each microcore contained the outermost xylem, cambial, and phloem tissues. All microcores were dehydrated successively in ethanol and D-limonene (Rossi et al., 2006). After that, microcores were embedded in paraffin and cut using a microtome to obtain a thin slice (7 μm thickness). The slice was stained with cresyl violet acetate (0.05% in water) and then observed with visible and polarized light at a magnification of 400× to identify the mature and immature xylem cells (Deslauriers et al., 2003). Stained immature xylem cells show a varying color from light to deep violet. The xylem cell could be identified as a mature cell when the violet was completely replaced by blue (Rossi et al., 2014). Magnified images of the outermost 50 mature xylem cell layers were taken under the microscope, and these images were used to calculate the cross-sectional areas of cells. Based on DBH increments and measured xylem cell diameters, *S. superba* and *C. chinensis* generate average of ~200 and ~140 mature tracheid layers within one year. The growing season in this experimental site was from April to October. Therefore, the outermost 50 mature xylem tracheid layers may generate within two or three months with similar climatic conditions, which provides the possibility to study the N addition effect on xylem cell size.

For each target tree, 100 mature xylem tracheid cells were randomly selected within the outermost 50 mature xylem tracheid layers to calculate the cross-sectional areas of the tracheid wall and the tracheid lumen using Adobe Photoshop CS6 software (Adobe, USA). On the other hand, vessels within the outermost 50 mature xylem tracheid layers were selected to calculate the cross-sectional vessel areas of target trees. Based on our microcore samples (only 2 mm width), there are more vessels for *S. superba* (>100 vessels) than those for *C. chinensis* (approximately 70–90 vessels) within the outermost 50 mature xylem tracheid layers. Therefore, for *S. superba*, we randomly selected 100 vessels within the outermost 50 mature xylem tracheid layers to calculate the cross-sectional vessel area. However, for *C. chinensis*, we selected all vessels within the outermost 50 mature xylem tracheid layers of the microcore to calculate the cross-sectional vessel area. In the magnified image, circular rings with a blue color represented the tracheid walls, and pink sections within circular rings represented the tracheid lumens (Fig. S1). Larger circular sections without blue-colored walls represented vessels. For the vessel, only the total cross-sectional area was calculated. For the broadleaf species, tracheid cells are majorly composed of fiber and can also be named as fibrous tracheid. Approximately 50% wood volume is taken up by fibrous tracheids in broadleaf trees, and approximately 30% wood volume is taken up by vessels (Xu, 2008). Tracheids within broadleaf trees provide mechanical support for wood and vessels supporting water transportation (Xu, 2008). Under the Photoshop environment, “Image-Adjust”, “Black & White”, “Filter-Sharpen”, and “Sharpen Edges” functions were used successively to modify the original photos and obtain images with two colors (black and white). After that, the “Magic Stick” function was used to select ranges of the tracheid wall, tracheid lumen, and vessel. After that, the pixel point numbers of selected ranges could be obtained. Areas of the tracheid wall, tracheid lumen, and vessel were calculated by transferring the pixel point numbers to areas based on image resolution. The average wall and lumen areas of the selected 100 tracheid cells were calculated to represent the cross-sectional areas of the tracheid wall and tracheid lumen for each target tree. An average area of selected vessels was calculated to represent the cross-sectional area of the vessel for each target tree.

A preliminary experiment had been conducted to differentiate tree ring boundaries of adjacent growing seasons for *S. superba* and *C. chinensis*, but the boundaries of the two species were fuzzy. In our study, reliable results could not be obtained in the preliminary experiment, and it was hard to investigate the N addition effect on the annual dynamic of xylem cell growth of these species by counting cell number or measuring tree ring width. Therefore, we focused on the effects of the N addition on xylem cell sizes by calculating the cross-sectional areas.

2.5. Statistical analysis

Statistical analysis was performed using the SPSS 18.0 software package for Windows (SPSS Inc., Chicago, IL, USA). Five treated plots within one block represent 5 treatments (CK, UAN25, UAN50, CAN25, and CAN50). Four blocks were set as 4 replicates. A two-way ANOVA with N addition approaches (CAN and UAN) and addition rates (0, 25, and 50 kg N ha^{-1} yr^{-1}) as the main factors was performed to test differences in sizes (tracheid wall, tracheid lumen, and vessel), DBH increments, photosynthetic rates, and cellulose $\delta^{13}C_{PDB}$ at $P < 0.05$ for *S. superba* and *C. chinensis*, and the Bonferroni method was used for post hoc analysis. For ANOVA tests of differences in sizes, photosynthetic rates, stomatal conductance, and cellulose $\delta^{13}C_{PDB}$, there were 4 *S. superba* and 4 *C. chinensis* in each treatment. For ANOVA tests of differences in DBH increments, 61 *S. superba* and 128 *C. chinensis* were divided into different treatments.

Table 1
Characteristics of *Schima superba* and *Castanopsis chinensis* in N manipulative experimental plots.

Tree species	Tree number	Diameter at breast height (cm)			Height (m)			Crown diameter (m)		
		Max	Mean	Min	Max	Mean	Min	Max	Mean	Min
Schima superba	61	52.6	22.4	7.8	22.5	16.1	8.0	9.0	5.4	1.5
Castanopsis chinensis	128	42.4	18.8	2.8	19.0	12.7	1.5	8.5	4.9	0.5

3. Results

3.1. Increment of diameter at breast height

In our experimental site, data of mean DBH, height, and crown diameter suggested that *S. superba* was commonly bigger in size compared to *C. chinensis* (Table 1). DBH increments (3 years) were 1.48 ± 0.98 and 0.63 ± 0.56 cm for *S. superba* and *C. chinensis*, respectively. As shown in Table S1, effects of N addition on DBH increments were insignificant, regardless of *S. superba* and *C. chinensis*. Meanwhile, tree sizes (initial DBH) were positively related with DBH increments of *S. superba* (R^2 = 0.44, $P < 0.001$) and *C. chinensis* (R^2 = 0.38, $P < 0.001$).

3.2. Photosynthetic rate, stomatal conductance, and cellulose $\delta^{13}C_{PDB}$

Results showed that photosynthetic rates, stomatal conductance, and cellulose $\delta^{13}C_{PDB}$ of *S. superba* and *C. chinensis* were not affected by N addition (Fig. 4 & S3). Photosynthetic rates of *S. superba* ranged from 2.98 to 7.41 μmol m^{-2} s^{-1} within different treatments. For *C. chinensis*, photosynthetic rates ranged from 1.78 to 6.03 μmol m^{-2} s^{-1} within different treatments. The stomatal conductance of *S. superba* ranged from 0.014 to 0.033 mmol m^{-2} s^{-1} within different treatments. For *C. chinensis*, stomatal conductance ranged from 0.012 to 0.029 mmol m^{-2} s^{-1} within different treatments. Cellulose $\delta^{13}C_{PDB}$ were −28.4 ± 0.34 and −27.8 ± 0.39 for *S. superba* and *C. chinensis*, respectively.

3.3. Xylem tracheid and vessel

Addition approaches (CAN and UAN) and addition rates (0, 25, and 50 kg N ha^{-1} yr^{-1}) showed inconsistent effects on xylem tracheid sizes for different tree species. For the cross-sectional areas of tracheid wall and lumen of *S. superba*, addition rates showed significant effects ($P < 0.01$), but effects of the addition approaches on cell sizes were insignificant (Fig. 2A, C). Linear relationships between tracheid areas and N addition rates were significant for *S. superba* ($P < 0.05$). For *S. superba*, CAN25 and UAN25 caused 4.03 ± 0.04% and3.63 ± 0.05% increase in tracheid size compared to CK, while CAN50 and UAN50 caused 8.67 ± 0.07% and 8.06 ± 0.07% increase in tracheid size compared to CK. For *C. chinensis*, the tracheid areas were significantly affected by N addition approaches ($P < 0.01$), but only UAN50 caused a significant increase in tracheid sizes (Fig. 2B, D). UAN50 caused 8.97 ± 0.06% and 9.39 ± 0.11% increase in areas of tracheid wall and tracheid lumen compared to CK. Vessel areas of both tree species were not affected by N addition ($P > 0.05$; Fig. 3), regardless of addition approaches or rates.

As shown in Fig. S2, proportions of tracheid wall area to lumen area were not affected by N addition, regardless of *S. superba* and *C. chinensis*. Proportions of the tracheid wall area to lumen area were 1.51 ± 0.16% for *S. superba*. For *C. chinensis*, proportions of the tracheid wall area to the lumen area were 1.15 ± 0.14%.

4. Discussion

4.1. N addition and xylem anatomy

In our study, 3 years exogenous N addition increased newly formed xylem tracheid size (3.09–11.79%; Fig. 2). This result was similar to those previous studies carried out in boreal forests (Beets et al., 2001; Makinen et al., 2002). Previous studies about the N effects on wood formation reported that N treatment could accelerate cell growth and promote holocellulose accumulation in the xylem, which lead to a thicker cell wall (Pitre et al., 2007; Pitre et al., 2010). Previous studies also

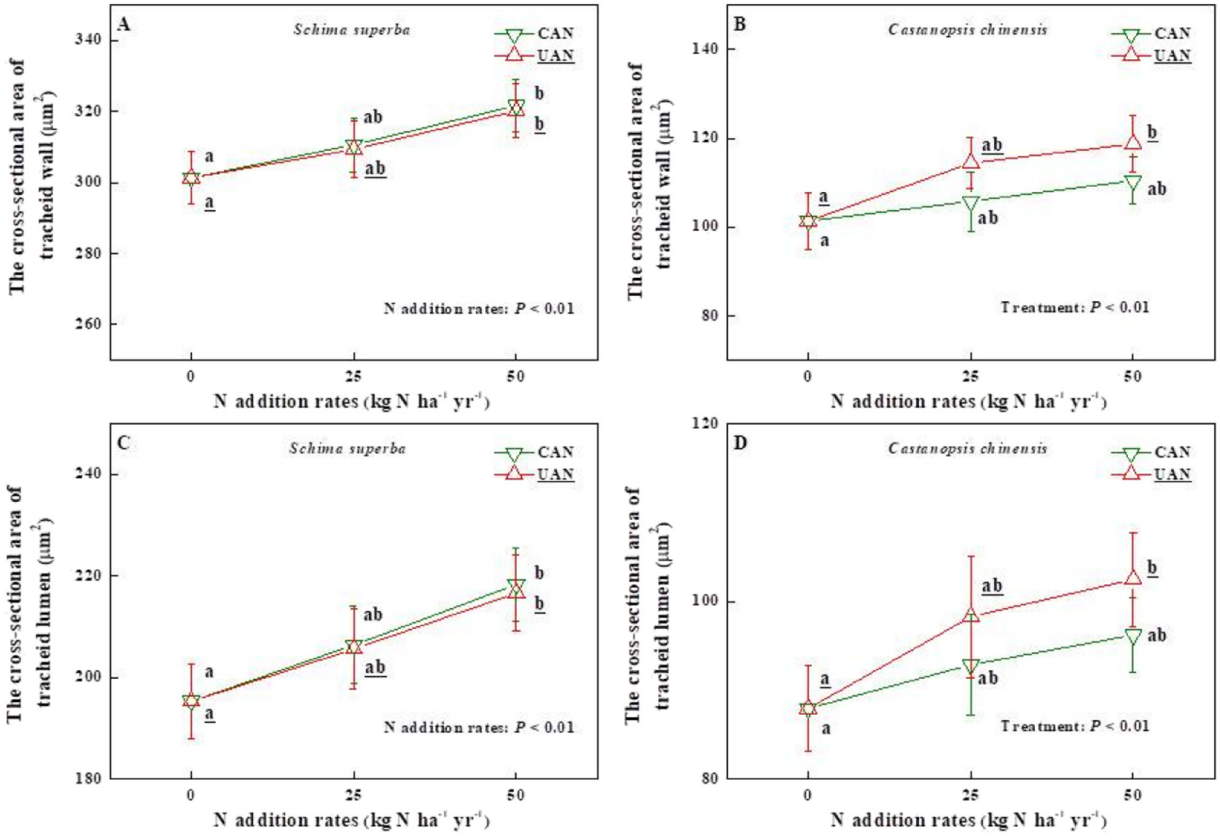

Fig. 2. The cross-sectional areas (μm²) of the tracheid wall and tracheid lumen of *Schima superba* and *Castanopsis chinensis* for different N addition approaches (CAN, canopy addition N; UAN, understory addition N) and N addition rates (0, 25, and 50 kg N ha^{-1} yr^{-1}). The lowercase letters with and without an underline indicate significant differences in the cross-sectional areas between different N addition rates at $P < 0.05$ for CAN and UAN, respectively. Significant effects from two-way ANOVA are shown on each panel (Bonferroni method, n = 4). Error bars represent standard deviation.

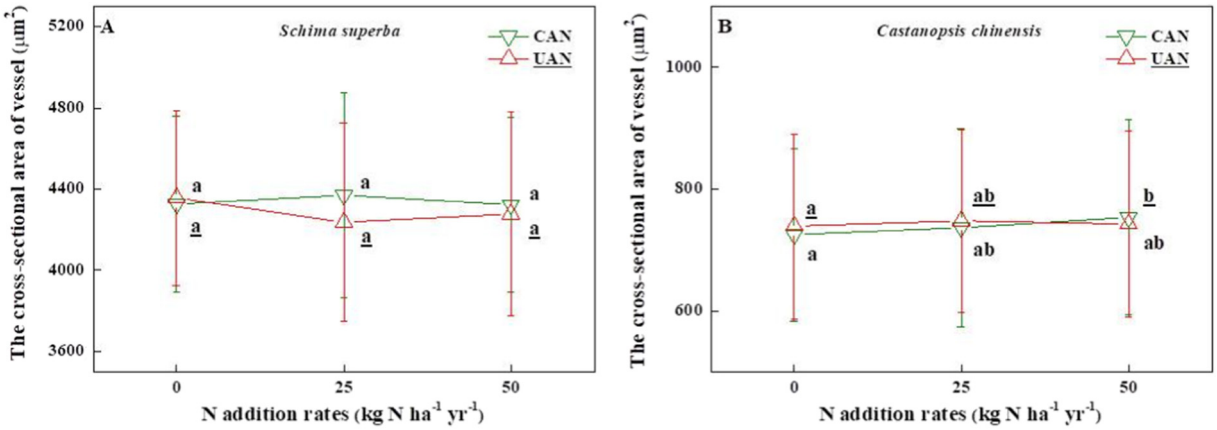

Fig. 3. The cross-sectional areas (μm^2) of vessel of *Schima superba* and *Castanopsis chinensis* for different N addition approaches (CAN, canopy addition N; UAN, understory addition N) and N addition rates (0, 25, and 50 kg N ha^{-1} yr^{-1}). The lowercase letters with and without an underline indicate significant differences in the cross-sectional areas between different N addition rates at $P < 0.05$ for CAN and UAN, respectively. Significant effects from two-way ANOVA are shown on each panel (Bonferroni method, n = 4). Error bars represent standard deviation.

reported that several genes related to secondary xylem wall deposition were differentially regulated by N availability (Plavcova et al., 2013; Camargo et al., 2014), indicating that changes in the xylem cell structure might be associated with differences in genes expression. N is considered as the limiting nutrient for plant growth, while N addition can be used to alter the quality and quantity of the tree lignocellulosic biomass. In this way, N is used to increase the productivity of commercial forests by the application of a large amount of N fertilizer (Xu et al., 2012). Wood recalcitrance to degradation is the main limitation for wood processing and economic benefit in the industry, and wood quality is highly dependent on the composition and structure of the tracheid wall (Mansfield et al., 2012; Mizrachi et al., 2012). Previous studies reported that N addition could lead to a wider vessel or thinner cell wall (Luo et al., 2005; Plavcova et al., 2013), suggesting that N addition might lead to a decline in wood hardness. However, in our study, proportions of the tracheid wall area to the lumen area and vessel sizes were not

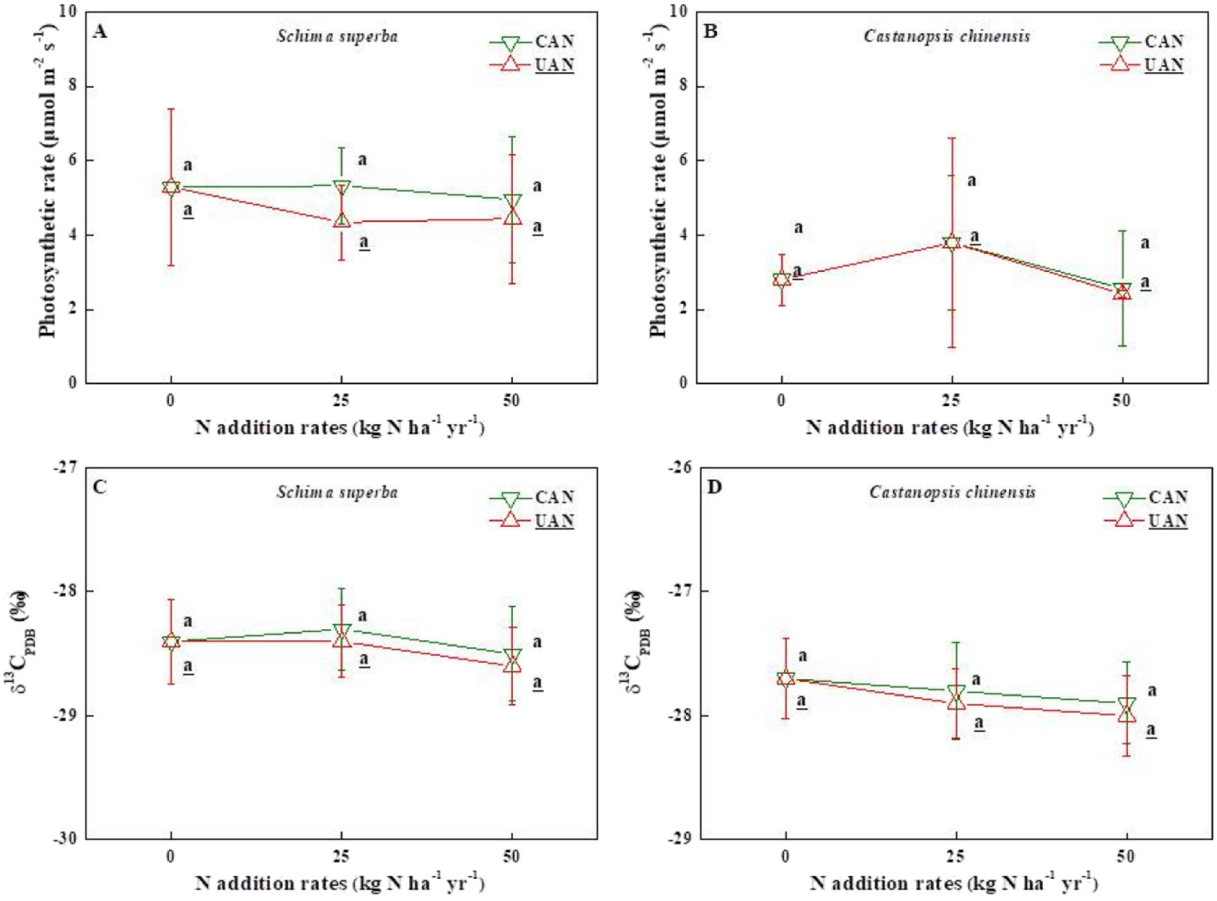

Fig. 4. Photosynthetic rates ($\mu mol\ m^{-2}\ s^{-1}$) and cellulose $\delta^{13}C_{PDB}$ (‰) of *Schima superba* and *Castanopsis chinensis* for different N addition approaches (CAN, canopy addition N; UAN, understory addition N) and N addition rates (0, 25, and 50 kg N ha^{-1} yr^{-1}). The lowercase letters with and without and underline indicate significant differences in photosynthetic rates and cellulose $\delta^{13}C_{PDB}$ between different N addition rates at $P < 0.05$ for CAN and UAN, respectively (Bonferroni method, n = 4). Error bars represent standard deviation.

affect by N addition (Fig. S2), suggesting that N addition might not affect the wood quality of the two subtropical broadleaf species we selected.

Effects of N addition on xylem tracheid size were dependent on N addition approaches (CAN and UAN). Naturally deposited N passes through the forest canopy before it reaches the floor, and canopy-retained N becomes immediately available for plant leaves and subsequently increases photosynthesis, which leads to production promotion (Rose, 1996; Wortman et al., 2012). A previous study reported that the forest canopy retained 20–25% of total atmospheric N deposition at N deposition rates of 25–40 kg N ha^{-1} yr^{-1} (Wortman et al., 2012). Canopy N retention is able to cause a decline in the amount and a change in the composition (variations of NH_4^+: NO_3^- ratios) of N reaching forest floor (Houle et al., 2015). The root N uptake from the soil environment is the dominant N source for tree growth, and a lower ratio of N input to soil may cause a lesser effect of N addition on tree growth. In this way, the effect of CAN on xylem anatomy should be less significant than that of UAN. According to our results, the xylem tracheid size of *C. chinensis* was not affected by CAN, suggesting that less N input to soil could limit the effect of N addition on *C. chinensis*. However, for *S. superba*, both CAN and UAN significantly increased xylem tracheid sizes ($P < 0.05$). Meanwhile, significantly linear relationships were also found between tracheid sizes and N addition rates for *S. superba*, regardless of the N addition approach used ($P < 0.05$). These findings suggested that effect of N addition on xylem tracheid size was dependent on tree species. Previous studies reported that canopy-retained N can also be taken up by canopy tree leaves and sequentially promote the production of canopy trees (Sparks, 2009; Wortman et al., 2012). *S. superba* is an upper canopy species that is commonly taller in height and bigger in size compared to *C. chinensis* (Table 1); therefore, canopy-retained N can be utilized by *S. superba* to promote xylem cell growth. On the other hand, although canopy N retention decreases N reaching the forest floor (Hanson and Lindberg, 1991; Sparks, 2009), *S. superba* is still available to obtain more deposited N from soil than other understory species through competition (Cortini et al., 2012; Jiang et al., 2016). In the subtropical forests of southern China, it has been reported that the intraspecific competition intensity of broadleaf tree species decreases gradually as tree diameter increases (Zhang et al., 2006), and *C. chinensis* commonly suffers more intensively interspecific competition from *S. superba* or other canopy tree species in water uptake and nutrient association (Li et al., 2013). In this way, N deposited from CAN treatment can still be taken in and utilized by *S. superba* more than *C. chinensis*, while deposited N will be less available for *C. chinensis* under the CAN treatment. Therefore, the tracheid size of *S. superba* was promoted under CAN, while CAN did not show any impact on the tracheid size of *C. chinensis*. For UAN, added N was sprayed uniformly to the ground and could be utilized by all biota in the forest. UAN may cause a consistent response of different species to N addition, while CAN may lead to contrasting results of the N effects for canopy and understory species. Therefore, the UAN experimental design may pose challenges for mechanistic understanding and forest dynamics projection in the future.

The change in xylem cell structure is related to tree hydraulic properties and water use efficiency. A previous study reported wider vessels and higher specific conductivities in the hybrid poplar under N addition (Hacke et al., 2010), and a more conductive xylem would be better able to support tree growth and leaf areas enhancement (Ouyang et al., 2017). However, N addition had an insignificant effect on vessel size, suggesting that tree hydraulic properties were not affected by N addition.

4.2. N addition and tree growth

Xylem formation plays a vital role in sequestering atmospheric CO_2 and is closely related to tree growth (Huang et al., 2014). In our study, DBH increments were measured to represent the tree radial growth. Briefly, the DBH increments of both tree species were only significantly affected by the tree sizes, whereas N addition approaches or addition rates showed insignificant impacts on DBH increments. These results suggested that tree growth was not affected by 3 years of N addition. Tropical or subtropical forests are commonly phosphorus-limited; therefore, tree C sequestration or tree growth commonly do not respond to N addition in these forests (Penuelas et al., 2013; Sitch et al., 2015).

In our study, xylem tracheid size and DBH increment were respectively promoted and unchanged under N addition (Fig, 2; Table S1), which seemed to be a conflict about the N effect on tree growth. One potential explanation is that the increase in tracheid size cannot be directly related to tree growth when the tracheid numbers are not counted. Another potential explanation is that xylem tracheid size is measured on the microscale, but DBH increment is obtained through a less precise measurement. In this way, a slight increase in tracheid size may not be reflected through DBH increment.

The short-term effects of N addition on wood formation, soil respiration, and tree growth had been reported in previous studies (Micks et al., 2004; Pitre et al., 2007; Mamashita et al., 2015). In this way, the positive effect of N addition on xylem tracheid size might also be a short-term phenomenon. In our study, only the tracheid size showed a significant response to 3 years of N addition, while other growth and water conductivity-related variables (such as vessel size, DBH increment, $\delta^{13}C_{PDB}$, and photosynthetic rates) did not show any significant responses. Therefore, it cannot be concluded that N addition will further increase the xylem tracheid size or tree growth of the broadleaf species of subtropical forests in the future. The wood cellulose $\delta^{13}C_{PDB}$ records the proportion of fixed C to the total assimilated C and is closely linked to photosynthetic capacity and stomatal regulation during the tree growth period (Ogee et al., 2009; Belmecheri et al., 2014). Therefore, wood cellulose $\delta^{13}C_{PDB}$ contains valuable records of past climate and C allocation within trees (Barbour et al., 2002). In our study, the cellulose $\delta^{13}C_{PDB}$ of two species were not affected by N addition (Fig. 4), suggesting that assimilated C allocation within the tree did not change under N addition. Photosynthetic rates and stomatal conductance also showed insignificant responses to N addition (Fig. 4), suggesting that the C input rates of two tree species might not be influenced by N addition. These results further indicated that the tree growth of subtropical dominant broadleaf species might not be affected by short-term N addition, but further investigation on the long-term effect was necessary.

5. Conclusions

Our findings suggested that the effects of N addition on xylem tracheid sizes were dependent on tree species and N addition approaches (CAN and UAN), and those results from the understory N addition approach should be reevaluated. N addition could change the xylem ultrastructure of the dominant broadleaf tree species in subtropical forests; however, vessel size and tree growth were not affected by short-term N addition. This information can be used to improve management practices in mitigating and preventing the likely impact of increasing atmospheric N deposition in subtropical forests.

Acknowledgement

This project was supported by the National Natural Science Foundation of China, Grant No. 31600435, 31570584, 31570585, and 31770487; the GDAS' Special Project of Science and Technology Development, Grant No. 2017GDASCX-0833; the 100 Talents Program of the Chinese Academy of Sciences (CAS), Grant No. Y421081001; the Project of Science and Technology Innovation Platform of Guangdong Province, China, Grant No. 2015B070701017; the Science and Technology Planning Project of Guangdong Province, Grant No. 2016B070701015, 2017A070702015. The authors thank Yuanqiu Li for sampling. The authors herein state that they have no conflicts of interest to declare.

Appendix A. Supplementary data

Supplementary data to this article can be found online at https://doi.org/10.1016/j.scitotenv.2018.06.133.

References

Arend, M., Fromm, J., 2007. Seasonal change in the drought response of wood cell development in poplar. Tree Physiol. 27, 985–992.

Barbour, M.M., Walcroft, A.S., Farquhar, G.D., 2002. Seasonal variation in delta C-13 and delta O-18 of cellulose from growth rings of *Pinus radiata*. Plant Cell Environ. 25, 1483–1499.

Beets, P.N., Gilchrist, K., Jeffreys, M.P., 2001. Wood density of radiata pine: effect of nitrogen supply. For. Ecol. Manag. 145, 173–180.

Belmecheri, S., Maxwell, R.S., Taylor, A.H., Davis, K.J., Freeman, K.H., Munger, W.J., 2014. Tree-ring $\delta^{13}C$ tracks flux tower ecosystem productivity estimates in a NE temperate forest. Environ. Res. Lett. 9, 074011.

Brookshire, E.N.J., Gerber, S., Menge, D.N.L., Hedin, L.O., 2012. Large losses of inorganic nitrogen from tropical rainforests suggest a lack of nitrogen limitation. Ecol. Lett. 15, 9–16.

Camargo, E.L.O., Nascimento, L.C., Soler, M., Salazar, M.M., Lepikson-Neto, J., Marques, W.L., et al., 2014. Contrasting nitrogen fertilization treatments impact xylem gene expression and secondary cell wall lignification in eucalyptus. BMC Plant Biol. 14, 17.

Cortini, F., Comeau, P.G., Bokalo, M., 2012. Trembling aspen competition and climate effects on white spruce growth in boreal mixtures of Western Canada. For. Ecol. Manag. 277, 67–73.

Dail, D.B., Hollinger, D.Y., Davidson, E.A., Fernandez, I., Sievering, H.C., Scott, N.A., et al., 2009. Distribution of nitrogen-15 tracers applied to the canopy of a mature spruce-hemlock stand, Howland, Maine, USA. Oecologia 160, 589–599.

Dao, M.C.E., Rossi, S., Walsh, D., Morin, H., Houle, D., 2015. A 6-year-long manipulation with soil warming and canopy nitrogen additions does not affect xylem phenology and cell production of mature black spruce. Front. Plant Sci. 6, 9.

Deslauriers, A., Morin, H., Begin, Y., 2003. Cellular phenology of annual ring formation of Abies balsamea in the Quebec boreal forest (Canada). Can. J. For. Res. 33, 190–200.

Findlay, S.E.G., 2005. Increased carbon transport in the Hudson River: unexpected consequence of nitrogen deposition? Front. Ecol. Environ. 3, 133–137.

Galloway, J.N., Cowling, E.B., 2002. Reactive nitrogen and the world: 200 years of change. Ambio 31, 64–71.

Hacke, U.G., Plavcova, L., Almeida-Rodriguez, A., King-Jones, S., Zhou, W.C., Cooke, J.E.K., 2010. Influence of nitrogen fertilization on xylem traits and aquaporin expression in stems of hybrid poplar. Tree Physiol. 30, 1016–1025.

Hanson, P.J., Lindberg, S.E., 1991. Dry deposition of reactive nitrogen-compounds - a review of leaf, canopy and non-foliar measurements. Atmos. Environ. 25, 1615–1634.

Hawkins, B.J., Davradou, M., Pier, D., Shortt, R., 1995. Frost hardiness and winter photosynthesis of thuja-plicata and pseudotsuga-menziesii seedlings grown at 3 rates of nitrogen and phosphorus supply. Can. J. For. Res. 25, 18–28.

Hedin, L.O., Brookshire, E.N.J., Menge, D.N.L., Barron, A.R., 2009. The nitrogen paradox in tropical forest ecosystems. Annu. Rev. Ecol. Evol. Syst. 40, 613–635 Annual Reviews, Palo Alto.

Hogberg, P., Fan, H.B., Quist, M., Binkley, D., Tamm, C.O., 2006. Tree growth and soil acidification in response to 30 years of experimental nitrogen loading on boreal forest. Glob. Chang. Biol. 12, 489–499.

Houle, D., Marty, C., Duchesne, L., 2015. Response of canopy nitrogen uptake to a rapid decrease in bulk nitrate deposition in two eastern Canadian boreal forests. Oecologia 177, 29–37.

Huang, J.G., Deslauriers, A., Rossi, S., 2014. Xylem formation can be modeled statistically as a function of primary growth and cambium activity. New Phytol. 203, 831–841.

Hutchison, J.S., Henry, H.A.L., 2010. Additive effects of warming and increased nitrogen deposition in a temperate old field: plant productivity and the importance of winter. Ecosystems 13, 661–672.

Ibanez, I., Zak, D.R., Burton, A.J., Pregitzer, K.S., 2016. Chronic nitrogen deposition alters tree allometric relationships: implications for biomass production and carbon storage. Ecol. Appl. 26, 913–925.

Jiang, X.Y., Huang, J.G., Stadt, K.J., Comeau, P.G., Chen, H.Y.H., 2016. Spatial climate-dependent growth response of boreal mixedwood forest in western Canada. Glob. Planet. Chang. 139, 141–150.

Kong, G.H., Huang, Z.L., Zhang, Q.M., Liu, S.Z., Mo, J.M., He, D.Q., 1997. Type, structure, dynamics and management of the lower subtropical evergreen broad-leafed forest in the Dinghushan Biosphere Reserve of China. Tropics 6, 335–350.

Lachenbruch, B., McCulloh, K.A., 2014. Traits, properties, and performance: how woody plants combine hydraulic and mechanical functions in a cell, tissue, or whole plant. New Phytol. 204, 747–764.

Li, Z., Hu, S., Li, W., Li, Q., 2013. Intra-specific and inter-specific competitions among major trees species in Pinus massoniana and *Schima superba* mixed forest in northeastern Guangdong Province. J. Cent. S. Univ. For. Technol. 33, 91–95 in Chinese with English abstract.

Liu, N., Guo, Q., 2012. Resource-use efficiencies of three indigenous tree species planted in resource islands created by shrubs: implications for reforestation of subtropical degraded shrublands. Plant Ecol. 213, 1177–1185.

Liu, N., Guo, Q., Ren, H., Sun, Z., 2016. *Schima superba* outperforms other tree species by changing foliar chemical composition and shortening construction payback time when facilitated by shrubs. Sci. Rep. 6, 19855.

Loader, N.J., Robertson, I., Barker, A.C., Switsur, V.R., Waterhouse, J.S., 1997. An improved technique for the batch processing of small wholewood samples to alpha-cellulose. Chem. Geol. 136, 313–317.

Lu, X.K., Mo, J.M., Gilliam, F.S., Zhou, G.Y., Fang, Y.T., 2010. Effects of experimental nitrogen additions on plant diversity in an old-growth tropical forest. Glob. Chang. Biol. 16, 2688–2700.

Lu, X., Gilliam, F.S., Yu, G., Li, L., Mao, Q., Chen, H., et al., 2013. Long-term nitrogen addition decreases carbon leaching in a nitrogen-rich forest ecosystem. Biogeosciences 10, 3931–3941.

Lu, X.K., Mao, Q.G., Gilliam, F.S., Luo, Y.Q., Mo, J.M., 2014. Nitrogen deposition contributes to soil acidification in tropical ecosystems. Glob. Chang. Biol. 20, 3790–3801.

Lu, X.K., Mao, Q.G., Mo, J.M., Gilliam, F.S., Zhou, G.Y., Luo, Y.Q., et al., 2015. Divergent responses of soil buffering capacity to long-term N deposition in three typical tropical forests with different land-use history. Environ. Sci. Technol. 49, 4072–4080.

Lukac, M., Calfapietra, C., Lagomarsino, A., Loreto, F., 2010. Global climate change and tree nutrition: effects of elevated CO2 and temperature. Tree Physiol. 30, 1209–1220.

Luo, Z.B., Langenfeld-Heyser, R., Calfapietra, C., Polle, A., 2005. Influence of free air CO2 enrichment (EUROFACE) and nitrogen fertilisation on the anatomy of juvenile wood of three poplar species after coppicing. Trees Struct. Funct. 19, 109–118.

MacDonald, J.A., Dise, N.B., Matzner, E., Armbruster, M., Gundersen, P., Forsius, M., 2002. Nitrogen input together with ecosystem nitrogen enrichment predict nitrate leaching from European forests. Glob. Chang. Biol. 8, 1028–1033.

Makinen, H., Saranpaa, P., Linder, S., 2002. Wood-density variation of Norway spruce in relation to nutrient optimization and fibre dimensions. Can. J. For. Res. 32, 185–194.

Mamashita, T., Larocque, G.R., DesRochers, A., Beaulieu, J., Thomas, B.R., Mosseler, A., et al., 2015. Short-term growth and morphological responses to nitrogen availability and plant density in hybrid poplars and willows. Biomass Bioenergy 81, 88–97.

Mansfield, S.D., Kang, K.Y., Chapple, C., 2012. Designed for deconstruction - poplar trees altered in cell wall lignification improve the efficacy of bioethanol production. New Phytol. 194, 91–101.

Matson, A.L., Corre, M.D., Veldkamp, E., 2014. Nitrogen cycling in canopy soils of tropical montane forests responds rapidly to indirect N and P fertilization. Glob. Chang. Biol. 20, 3802–3813.

May, J.D., Burdette, S.B., Gilliam, F.S., Adams, M.B., 2005. Interspecific divergence in foliar nutrient dynamics and stem growth in a temperate forest in response to chronic nitrogen inputs. Can. J. For. Res. 35, 1023–1030.

Micks, P., Aber, J.D., Boone, R.D., Davidson, E.A., 2004. Short-term soil respiration and nitrogen immobilization response to nitrogen applications in control and nitrogen-enriched temperate forests. For. Ecol. Manag. 196, 57–70.

Mizrachi, E., Mansfield, S.D., Myburg, A.A., 2012. Cellulose factories: advancing bioenergy production from forest trees. New Phytol. 194, 54–62.

Mo, J.M., Li, D.J., Gundersen, P., 2008. Seedling growth response of two tropical tree species to nitrogen deposition in southern China. Eur. J. For. Res. 127, 275–283.

Ogee, J., Barbour, M.M., Wingate, L., Bert, D., Bosc, A., Stievenard, M., et al., 2009. A single-substrate model to interpret intra-annual stable isotope signals in tree-ring cellulose. Plant Cell Environ. 32, 1071–1090.

Onoda, Y., Richards, A.E., Westoby, M., 2010. The relationship between stem biomechanics and wood density is modified by rainfall in 32 Australian woody plant species. New Phytol. 185, 493–501.

Ouyang, L., Zhao, P., Zhu, L.W., Zhang, Z.Z., Zhao, X.H., Ni, G.Y., 2017. Difference in response of water use to evaporative demand for codominant diffuse-porous versus ring-porous tree species under N addition in a temperate forest. Ecohydrology 10, 9.

Penuelas, J., Poulter, B., Sardans, J., Ciais, P., van der Velde, M., Bopp, L., et al., 2013. Human-induced nitrogen-phosphorus imbalances alter natural and managed ecosystems across the globe. Nat. Commun. 4, 10.

Pitre, F.E., Cooke, J.E.K., Mackay, J.J., 2007. Short-term effects of nitrogen availability on wood formation and fibre properties in hybrid poplar. Trees Struct. Funct. 21, 249–259.

Pitre, F.E., Lafarguette, F., Boyle, B., Pavy, N., Caron, S., Dallaire, N., et al., 2010. High nitrogen fertilization and stem leaning have overlapping effects on wood formation in poplar but invoke largely distinct molecular pathways. Tree Physiol. 30, 1273–1289.

Plavcova, L., Hacke, U.G., Almeida-Rodriguez, A.M., Li, E.Y., Douglas, C.J., 2013. Gene expression patterns underlying changes in xylem structure and function in response to increased nitrogen availability in hybrid poplar. Plant Cell Environ. 36, 186–199.

Pratt, R.B., Jacobsen, A.L., Ewers, F.W., Davis, S.D., 2007. Relationships among xylem transport, biomechanics and storage in stems and roots of nine Rhamnaceae species of the California chaparral. New Phytol. 174, 787–798.

Rose, C.L., 1996. Forest canopy atmosphere interactions. Northwest Sci. 70, 7–14.

Rossi, S., Anfodillo, T., Menardi, R., 2006. Trephor: a new tool for sampling microcores from tree stems. IAWA J. 27, 89–97.

Rossi, S., Girard, M.J., Morin, H., 2014. Lengthening of the duration of xylogenesis engenders disproportionate increases in xylem production. Glob. Chang. Biol. 20, 2261–2271.

Rossi, S., Anfodillo, T., Cufar, K., Cuny, H.E., Deslauriers, A., Fonti, P., et al., 2016. Pattern of xylem phenology in conifers of cold ecosystems at the Northern Hemisphere. Glob. Chang. Biol. 22, 3804–3813.

Samuels, A.L., Kaneda, M., Rensing, K.H., 2006. The cell biology of wood formation: from cambial divisions to mature secondary xylem. Can. J. Bot. 84, 631–639.

Santini, N.S., Cleverly, J., Faux, R., Lestrange, C., Rumman, R., Eamus, D., 2016. Xylem traits and water-use efficiency of woody species co-occurring in the Ti Tree Basin arid zone. Trees Struct. Funct. 30, 295–303.

Sitch, S., Friedlingstein, P., Gruber, N., Jones, S.D., Murray-Tortarolo, G., Ahlstrom, A., et al., 2015. Recent trends and drivers of regional sources and sinks of carbon dioxide. Biogeosciences 12, 653–679.

Sparks, J.P., 2009. Ecological ramifications of the direct foliar uptake of nitrogen. Oecologia 159, 1–13.

Talhelm, A.F., Burton, A.J., Pregitzer, K.S., Campione, M.A., 2013. Chronic nitrogen deposition reduces the abundance of dominant forest understory and groundcover species. For. Ecol. Manag. 293, 39–48.
Thomas, R.Q., Canham, C.D., Weathers, K.C., Goodale, C.L., 2010. Increased tree carbon storage in response to nitrogen deposition in the US. Nat. Geosci. 3, 13–17.
Townsend, A.R., Cleveland, C.C., Houlton, B.Z., Alden, C.B., White, J.W.C., 2011. Multi-element regulation of the tropical forest carbon cycle. Front. Ecol. Environ. 9, 9–17.
Wortman, E., Tomaszewski, T., Waldner, P., Schleppi, P., Thimonier, A., Eugster, W., et al., 2012. Atmospheric nitrogen deposition and canopy retention influences on photosynthetic performance at two high nitrogen deposition Swiss forests. Tellus Ser. B Chem. Phys. Meteorol. 64, 14.
Wright, S.J., Yavitt, J.B., Wurzburger, N., Turner, B.L., Tanner, E.V.J., Sayer, E.J., et al., 2011. Potassium, phosphorus, or nitrogen limit root allocation, tree growth, or litter production in a lowland tropical forest. Ecology 92, 1616–1625.
Xu, Y., 2008. Xylology. China Forestry Publishing Company, Beijing, China.
Xu, G.H., Fan, X.R., Miller, A.J., 2012. Plant nitrogen assimilation and use efficiency. In: Merchant, S.S. (Ed.), Annual Review of Plant Biology. vol. 63. 63. Annual Reviews, Palo Alto, pp. 153–182.
Zhang, C., Huang, Z., Li, J., Shi, J., Li, L., 2006. Quantitative relationships of intra- and interspecific competition in Cryptocarya concinna. J. Appl. Ecol. 17, 22–26 (in Chinese with English abstract).
Zhang, W., Shen, W., Zhu, S., Wan, S., Luo, Y., Yan, J., et al., 2015. Can canopy addition of nitrogen better illustrate the effect of atmospheric nitrogen deposition on forest ecosystem? Sci. Rep. 5, 11245.
Zhao, C.Z., Liu, Q., 2009. Growth and photosynthetic responses of two coniferous species to experimental warming and nitrogen fertilization. Can. J. For. Res. 39, 1–11.